2009

Effect of the Regiochemistry of Butyl Amide Substituents on the Solution-State Structures of Lanthanide(III) DOTA-Tetraamide Complexes

Tomoyasu Mani
University of Texas at Dallas

Gyula Tircsó
University of Texas at Dallas

Piyu Zhao
University of Texas at Dallas

A. Dean Sherry
University of Texas at Dallas

Mark Woods
Portland State University, mark.woods@pdx.edu

Citation Details

Published as: Mani, T., Tircsó, G., Zhao, P., Sherry, A. D., & Woods, M. (2009). Effect of the regiochemistry of butyl amide substituents on the solution-state structures of lanthanide(III) DOTA-tetraamide complexes. Inorganic chemistry, 48(21), 10338–10345. https://doi.org/10.1021/ic9017008

Published in final edited form as:
Inorg Chem. 2009 November 2; 48(21): 10338–10345. doi:10.1021/ic9017008.

The Effect of the Regiochemistry of Butyl Amide Substituents on the Solution-State Structures of Lanthanide(III) DOTA-tetraamide complexes

Tomoyasu Mani[†], **Gyula Tircsó**[†,¬], **Piyu Zhao**[†], **A. Dean Sherry**[†,‰], and **Mark Woods**[‡,§,*]

[†]Department of Chemistry, University of Texas at Dallas, 800 W. Campbell Road, Richardson, TX 75080, UNITED STATES.

[‰]Advanced Imaging Research Center, UT Southwestern Medical Center, 5323 Harry Hines Blvd, Dallas, TX, 75235, UNITED STATES.

[†]Advanced Imaging Research Center, Oregon Health and Science Univeristy, 3181 SW Sam Jackson Park Road, Portland, OR, 97239, UNITED STATES.

[§]Department of Chemistry, Portland State University, 1719 SW 10th Avenue. Portland, OR 97201, UNITED STATES.

Abstract

The coordination geometry adopted by the lanthanide complexes of DOTA-tetraamides is a critical factor in determining their water exchange kinetics. Controlling the water exchange kinetics of DOTA-tetraamide complexes, and by extension their coordination geometry, is of particular interest because of the potential application of this class of complex as PARACEST MRI contrast agents. In order to facilitate the maximum CEST effect at the lowest pre-saturation powers much slower exchange kinetics are required than are commonly observed with these types of complex. Complexes that adopt the more slowly exchanging square antiprismatic coordination geometry are therefore preferred; however, the factors that govern which coordination geometry is preferred remain unclear. A series of DOTA-tetraamide complexes with butyl amide substituents in different regioisomeric configurations provides some insight into these factors. The population of each coordination geometry was found to vary substantially depending upon the regiochemistry of the butyl amide substituent. Unusually for DOTA-tetraamide complexes it was observed that the twisted square antiprismatic coordination geometry, usually favoured by early lanthanides, is also increasingly favoured by the later lanthanide ions. This is in marked contrast to simple DOTA-tetraamide complexes such as DOTAM. This effect becomes more prevalent the more bulky and more electron donating the amide butyl substituents become. It is also associated with loss of an inner-sphere water molecule from the complexes of later lanthanides that adopt the twisted square antiprismatic geometry. The complexes with *sec*-butyl substituents are inherently more complicated because of the introduction of a stereochemical centre into each pendant arm. Unlike chiral complexes with larger amide substituents there is no ‘locking’ effect of the orientation of the pendant arms in these complexes and up to four diastereoisomeric coordination isomers can be observed.

Phone: + 1 503 725 8238, Fax: + 1 503 7259525, mark.woods@pdx.edu, woodsmar@ohsu.edu.
[¬]Current address: Department of Inorganic and Analytical Chemistry, University of Debrecen, P.O. Box 21, Egyetem tér 1, Debrecen H-4010, Hungary.

Supporting Information Available: COSY spectrum of Yb-*RRRR-sec*-**1**. This material is available free of charge via the Internet at http://pubs.acs.org.

Keywords

Lanthanide complexes; coordination geometry; macrocyclic ligands; MRI contrast agents

Introduction

Interest in the chemistry of complexes formed between Ln^{3+} ions and macrocyclic ligands derived from DOTA (Chart 1) has largely been stimulated by the potential application of these complexes as MRI contrast agents.[1, 2] Although initially dismissed for this role because of their slow water exchange kinetics,[3–5] interest in DOTA-tetraamide ligands has recently experienced an upsurge.[6–20] This is primarily because the slow water exchange kinetics observed in DOTA-tetraamide complexes can be turned to advantage when they are employed as paramagnetic chemical exchange saturation transfer (ParaCEST) agents.[6] It has long been understood that controlling the rate of water exchange in lanthanide complexes is an extremely important goal for improving the effectiveness of contrast media. However, until the emergence of ParaCEST, nearly a decade ago, it had always been assumed that accelerating water exchange was the goal. Since ParaCEST agents rely upon slow water exchange kinetics, and theory suggests that extremely slow water exchange is most advantageous,[6, 21] it is now important to consider how water exchange can also be decelerated.

In Ln^{3+} complexes of DOTA and its derivatives one of the most important factors governing water exchange is the coordination geometry of the complex.[5, 22–25] These complexes are known to adopt two coordination geometries: a mono-capped square antiprism (SAP) and a mono-capped twisted square antiprism (TSAP).[26–29] A coordinated water molecule caps the antiprism in aqueous solution,[28] although it should be noted that for later lanthanides there is some evidence that the TSAP form is in fact a straight twisted square antiprism with no capping water molecule.[28, 30] It is now well established that the rate of water exchange in the TSAP isomer is between a factor of 10 and a factor of 50 faster than that of the SAP isomer.[5, 22–25] This has obvious implications for contrast agent design. If one is attempting to prepare a more effective Gd^{3+}-based T_1-shortening contrast agent in which fast exchange is preferred then it is preferable to have a complex that adopts a TSAP coordination geometry. Examples of how this can be achieved have been published.[24, 25] In contrast, a paraCEST agent ought to adopt a SAP coordination geometry as this will afford the slowest water exchange rates.

In solution the SAP and TSAP isomers are in dynamic exchange, interconverting by rotation of the pendant arms or through a flip in the conformation of the macrocyclic ring.[27–29, 31] In consequence both coordination geometries are accessible in solution and most usually both isomers are observed in solution. Because both exchange processes are normally slow on the NMR-timescale (rate constants are typically ~10 s^{-1})[29] the population of each coordination isomer can be determined by ^1H NMR. However, the factors that govern the distribution of the two coordination isomers in solution remain unclear. It is known that the earlier, larger Ln^{3+} ions tend to exhibit a marked preference for the TSAP isomer as this coordination geometry affords more space within the coordination cage.[30, 32, 33] In contrast the later lanthanides, which are smaller in size, tend to prefer a SAP geometry. However, for a given Ln^{3+} ion the ratio of SAP and TSAP isomers that are observed in solution is not a constant for all DOTA-tetraamide ligands. Indeed, the nature of the amide substituent appears to heavily influence this population distribution. This is readily seen in the series of simple DOTA-tetraamides: DOTAM, DTMA and DOTTA, where the amide substituents are NH_2, NHMe and NMe_2, respectively.[5] For Eu^{3+} the isomeric ratios, SAP:TSAP, are 4:1 for DOTAM, 3.2:1 for DTMA and 1:2 for DOTTA. However, when much larger amide substituents are employed, such as aromatic groups[34] or acetates[35] then it is generally observed that the SAP isomer dominates. Usually when these large substituents are employed the amount of TSAP isomer

present is so small that it cannot be detected by NMR. Nonetheless, it should be noted that a certain amount of TSAP isomer must be present because the exchange processes that interconvert these complexes are not halted in such systems and each motion, ring flip or arm rotation, will render a SAP isomer into a TSAP isomer.

If more effective ParaCEST agents are to be designed then it is important to understand the factors that govern the proportions of the SAP and TSAP isomers of given lanthanide DOTA-tetraamide complex. As part of a broader investigation into these parameters we have investigated the behaviour of four isomeric DOTA-tetraamide derivatives with butyl amide substituents. The regiochemistry of the butyl groups was systematically varied to afford *tert*-**1**, *iso*-**1**, *n*-**1** and the chiral *sec*-**1** (Chart1).

Experimental

General Remarks

All solvents and reagents were purchased from commercial sources and used as received unless otherwise stated. ^{1}H and ^{13}C NMR spectra were recorded on a Bruker Avance III spectrometer operating at 400.13 and 100.62 MHz, respectively or a JOEL Eclipse 270 spectrometer operating at 270.17 and 67.5 MHz, respectively. COSY and EXSY spectra were recorded on a Varian INOVA 500 spectrometer operating at 499.99 MHz. Infrared spectra were recorded on a Nicolet Avatar 360 FTIR spectrophotometer. Melting points were determined on a Fisher Johns melting point apparatus and are uncorrected. *iso*-**2** was prepared by previously published methods.[36]

Synthesis

***N-tert*-butyl bromoacetamide (*tert*-2)—**To a solution of *tert*-butylamine (10.0 g, 137 mmol) in dichloromethane (250 mL) was added potassium carbonate (37.8 g, 273 mmol) and the resulting suspension cooled to 0 °C. Bromoacetyl bromide (13.1 mL, 150 mmol) was added drop-wise with stirring over a period of half an hour. The reaction mixture was stirred at room temperature for 2 hours and then quenched with water (200 mL). The reaction mixture was transferred to a separatory funnel and the two phases were separated. The organic phase was washed with a 5% citric acid solution (200 mL) and water (200 mL), dried (Na_2SO_4) and the solvents were removed *in vacuo*. The solid residue was dried under vacuum to afford the title compound as a colorless solid (23.1 g, 87 %); mp: 76 – 78 °C. ^{1}H NMR (270MHz, $CDCl_3$): δ = 1.32 (9H, s, C($C\underline{H}_3$)$_3$), 3.73 (2H, s, Br$C\underline{H}_2CO$), 6.31 (1H, s br, NH); ^{13}C NMR (67.5 MHz, $CDCl_3$): δ = 28.5 (C($\underline{C}H_3$)$_3$), 29.9 ($\underline{C}(CH_3)_3$), 51.9 (Br$\underline{C}H_2CO$), 164.6 ($\underline{C}$=O); ν_{max}/cm^{-1} (KBr Disc): 3309 (NH), 3074, 3011, 2977, 2931, 2869, 1679 (C=O), 1651 (C=O), 1551, 1476, 1452, 1426, 1389, 1359, 1320, 1208, 1141, 934, 779, 676, 653, 575; Anal found C, 37.2; H, 6.2; N, 7.1 $C_6H_{12}BrNO$ requires C, 37.1; H, 6.2; N, 7.2.

***(R)-N-sec*-butyl bromoacetamide (*sec*-2)—**The title compound was prepared in an analogous manner to that described for *tert*-**2** using *(R)-sec*-Butylamine (5.0 g, 68 mmol) and was obtained as a colourless solid (11.2 g, 84 %); mp: 57 – 58 °C; ^{1}H NMR (400 MHz, $CDCl_3$): δ = 0.935 (3H, t, $^{3}J_{H\text{-}H}$ 8 Hz, CH(CH_3)$CH_2C\underline{H}_3$), 1.17 (3H, d, $^{3}J_{H\text{-}H}$ 6 Hz, CH($C\underline{H}_3$)CH_2CH_3), 1.49 (2H, dq, $^{3}J_{H\text{-}H}$ 8 Hz, $^{3}J_{H\text{-}H}$ 8 Hz, $C\underline{H}_2CH_3$), 3.91 (1H, m, $C\underline{H}(CH_3)CH_2CH_3$), 3.88 (2H, s, Br$C\underline{H}_2CO$), 6.23 (1H, s br, NH); ^{13}C NMR (100 MHz, $CDCl_3$): δ = 10.2 ($CH_2\underline{C}H_3$), 20.1 ($CH(\underline{C}H_3)CH_2CH_3$), 29.4 ($\underline{C}H_2CH_3$), 29.5 (Br$\underline{C}H_2CO$), 47.5 ($\underline{C}H(CH_3)CH_2CH_3$), 164.5 (C=O). ν_{max}/cm^{-1} (KBr Disc): 3280 (NH), 3080, 3022, 2969, 2932, 2875, 1646 (C=O), 1558, 1452, 1426, 1380, 1347, 1315, 1260, 1214, 1158, 1111, 975, 926, 889, 781, 759, 712, 653, 567; Anal found C, 37.2; H, 6.2; N, 7.2 $C_6H_{12}BrNO$ requires C, 37.1; H, 6.2; N, 7.2.

***N-n*-butyl bromoacetamide (*n*-2)—**The title compound was prepared in an analogous manner to that described for *tert*-**2** using *n*-butylamine (5.0 g, 68 mmol) and was obtained as a colourless solid (10.9 g, 82 %); mp 35 – 37 °C; ^{1}H NMR (400 MHz, $CDCl_3$): δ = 0.91 (3H, t, $^3J_{H\text{-}H}$ 7 Hz, $CH_2CH_2CH_2C\underline{H}_3$), 1.31 (2H, tq, $^3J_{H\text{-}H}$ 7 Hz, $^3J_{H\text{-}H}$ 7 Hz, $CH_2CH_2C\underline{H}_2CH_3$), 1.48 (2H, tt, $^3J_{H\text{-}H}$ 7 Hz, $^3J_{H\text{-}H}$ 7 Hz, $CH_2C\underline{H}_2CH_2CH_3$), 3.25 (2H, dt, $^3J_{H\text{-}H}$ 6 Hz, $^3J_{H\text{-}H}$ 7 Hz, $NHC\underline{H}_2CH_2$), 3.87 (2H, s, $BrC\underline{H}_2CO$), 6.57 (1H, s br, NH); ^{13}C NMR (400 MHz, $CDCl_3$): δ = 13.7 ($CH_2CH_2CH_2\underline{C}H_3$), 19.9 ($CH_2CH_2\underline{C}H_2CH_3$), 29.3 ($CH_2\underline{C}H_2CH_2CH_3$), 31.3 ($NH\underline{C}H_2CH_2$), 39.9 ($BrCH_2CO$), 165.3 (C=O); ν_{max}/cm^{-1} (KBr Disc): 3288 (NH), 3085, 2960, 2933, 2873, 1654 (C=O), 1599, 1466, 1437, 1382, 1310, 1212, 1151, 1079, 985, 886, 698, 554; Anal found C, 37.2; H, 6.1; N, 7.1 $C_6H_{12}BrNO$ requires C, 37.1; H, 6.2; N, 7.2.

Tetrakis-(*N-tert*-butyl)-1,4,7,10-tetraazacyclododecane-1,4,7,10-tetraacetamide (*tert*-1)—Under a nitrogen atmosphere at ambient temperature potassium carbonate (13.93 g, 101 mmol) was added to a solution of 1,4,7,10-tetraazacyclododecane (2.17 g, 12.6 mmol) and *tert*-**2** (9.98 g, 50 mmol) in anhydrous acetonitrile (200mL). The reaction mixture was stirred at 65 °C for 48 hours. After cooling the inorganic salts were removed by filtration and the solvents were removed *in vacuo*. The residue was taken up in hot methanol (200 mL) and filtered. The solvents were removed *in vacuo* and the residue washed with ice-cold water to afford a solid which was dried under vacuum and recrystallized from acetonitrile to afford the title compound as a colorless solid (8.08 g, 91 %); mp: 222 – 224 °C; ^{1}H NMR (270 MHz, CD_3OD): δ = 1.32 (36H, s, $C(C\underline{H}_3)_3$), 2.90 (16H, s br, ring $NC\underline{H}_2$), 3.30 (8H, s, $NC\underline{H}_2CO$); ^{13}C NMR (67.5 MHz, CD_3OD): δ = 27.7 ($C(\underline{C}H_3)_3$), 50.3 (ring $N\underline{C}H_2$), 50.6 ($\underline{C}(CH_3)_3$), 58.1 ($N\underline{C}H_2CO$), 170.8 (C=O); δ_{max}/cm^{-1} (KBr Disc): 3513 (NH), 3284 (NH), 3053, 2968, 2933, 2823, 1673 (C=O), 1537, 1456, 1393, 1367, 1308, 1226, 1101, 1024, 952, 591; *m/z* (ESI-MS+): 626 ($[M+H]^+$, 6%), 648 ($[M+Na]^+$, 4%), 664 ($[M+K]^+$, 100%); Anal Found C, 49.4; H, 8.6; N, 13.8 $C_{32}H_{64}N_8O_4{\cdot}KBr{\cdot}2.2H_2O$ requires C, 49.1; H, 8.8; N, 14.3.

Tetrakis-(*N-iso*-butyl)-1,4,7,10-tetraazacyclododecane-1,4,7,10-tetraacetamide (*iso*-1)—The title compound was prepared in an analogous manner to that described for *tert*-**1** using *iso*-**2** (6.0 g, 31 mmol) and was obtained as a colourless solid (15.1 g, 78 %); mp: 222 – 224 °C; ^{1}H NMR (400 MHz, $CDCl_3$): δ = 0.85 (12H, d, $^3J_{H\text{-}H}$ 7 Hz $CH_2CH(C\underline{H}_3)_2$), 1.53 (8H, m, $C\underline{H}_2CH(CH_3)_2$), 1.73 (4H, m, $CH_2C\underline{H}(CH_3)_2$), 2.64 (16H, s br, ring $NC\underline{H}_2$), 3.01 (8H, s, $NC\underline{H}_2CO$), 6.89 (4H, s br, NH); ^{13}C NMR (100 MHz, $CDCl_3$): δ = 20.2 ($CH_2CH(\underline{C}H_3)_2$), 30.9 ($CH_2\underline{C}H(CH_3)_2$), 46.6 ($\underline{C}H_2CH(CH_3)_2$), 53.5 (ring $N\underline{C}H_2$), 59.6 ($N\underline{C}H_2CO$), 170.5 (C=O); ν_{max}/cm^{-1} (KBr Disc): 3317 (NH), 3231 (NH), 3051, 2957, 2930, 2871, 2822, 1658 (C=O), 1542, 1468, 1453, 1388, 1363, 1333, 1301, 1259, 1207, 1161, 1143, 1103, 1064, 1001, 979, 963, 933, 915, 819, 801, 719, 573; *m/z* (ESI-MS+): 626 ($[M+H]^+$, 21%), 648 ($[M+Na]^+$, 30%), 664 ($[M+K]^+$, 100%); Anal Found C 61.2, H 10.3, N 17.6, $C_{32}H_{64}N_8O_4$ requires C, 61.5; H, 10.3; N, 17.9.

(*RRRR*)-Tetrakis-(*N-sec*-butyl)-1,4,7,10-tetraazacyclododecane-1,4,7,10-tetraacetamide (*RRRR-sec*-1)—The title compound was prepared in an analogous manner to that described for *tert*-**1** using *sec*-**2** (4.6 g, 24 mmol) and was obtained as a colourless solid (1.5 g, 47 %); mp: 202 – 204 °C; ^{1}H NMR (400 MHz, $CDCl_3$): δ = 0.82 (12H, t, $^3J_{H\text{-}H}$ 8 Hz $CH_2C\underline{H}_3$), 1.07 (12H, d, $^3J_{H\text{-}H}$ 7 Hz, $CHC\underline{H}_3$), 1.40 (8H, m, $C\underline{H}_2CH_3$), 2.68 (16H, s br, ring $NC\underline{H}_2$), 2.99 (8H, s, $NC\underline{H}_2CO$), 3.80 (4H, m, $NHC\underline{H}$), 6.56 (4H, s br, NH); ^{13}C NMR (100 MHz, $CDCl_3$): δ = 11.0 ($CH_2\underline{C}H_3$), 20.6 ($CH(\underline{C}H_3)CH_2CH_3$), 30.5 ($\underline{C}H_2CH_3$), 47.8 (ring $N\underline{C}H_2$), 59.2 ($N\underline{C}H_2CO$), 172.0 (C=O); ν_{max}/cm^{-1} (KBr Disc): 3434 (NH), 3256 (NH), 3057, 2969, 2933, 2876, 2820, 1669 (C=O), 1540, 1456, 1367, 1309, 1273, 1230, 1156, 1104, 948, 732; *m/z* (ESI-MS+): 626 ($[M+H]^+$, 28%), 648 ($[M+Na]^+$, 100%), 664($[M+K]^+$, 8%); Anal Found C 50.6, H 8.5, N 14.5, $C_{32}H_{64}N_8O_4{\cdot}KBr{\cdot}H_2O$ requires C, 50.4; H, 8.7; N, 14.7.

Tetrakis-(*N*-*n*-butyl)-1,4,7,10-tetraazacyclododecane-1,4,7,10-tetraacetamide (*n*-1)—The title compound was prepared in an analogous manner to that described for *tert*-**1** using *n*-**2** (4.6 g, 24 mmol) and was obtained as a colourless solid (2.1 g, 58 %); mp: 152 – 154 °C; ^{1}HNMR (400 MHz, CD_3OD): δ = 0.95 (12H, t, $^3J_{H\text{-}H}$ 8, Hz $CH_2CH_2CH_2C\underline{H}_3$), 1.35 (8H, tt, $^3J_{H\text{-}H}$ 6 Hz, $^3J_{H\text{-}H}$ 8 Hz, $CH_2CH_2C\underline{H}_2CH_3$), 1.52 (8H, tt, $^3J_{H\text{-}H}$ 6 Hz, $^3J_{H\text{-}H}$ 7 Hz, $CH_2C\underline{H}_2CH_2CH_3$), 2.73 (16H, s br, ring $NC\underline{H}_2$), 3.09 (8H, s, $NC\underline{H}_2CO$), 3.24 (8H, t, $^3J_{H\text{-}H}$ 7 Hz, $NHC\underline{H}_2$); ^{13}C NMR (100 MHz, CD_3OD): δ = 14.2 ($CH_2CH_2CH_2\underline{C}H_3$), 22.2 ($CH_2CH_2\underline{C}H_2CH_3$), 32.8 ($CH_2\underline{C}H_2CH_2CH_3$), 40.0 ($\underline{C}H_2CH_2CH_2CH_3$), 54.8 (ring $N\underline{C}H_2$), 59.8 ($N\underline{C}H_2CO$), 173.6 (C=O); ν_{max}/cm^{-1} (KBr Disc): 3299 (NH), 3244 (NH), 3077, 2958, 2932, 2873, 2859, 2817, 1660 (C=O), 1553, 1465, 1361, 1329, 1299, 1275, 1256, 1203, 1142, 1099, 1045, 1001, 981, 915, 888, 719, 569; *m/z* (ESI-MS+): 626 ($[M+H]^+$, 100%), 648 ($[M+Na]^+$, 78%); Anal Found C 58.4, H 9.9, N 16.7, $C_{32}H_{64}N_8O_4\cdot0.3KBr$ requires C, 58.2; H, 9.8; N, 17.0.

General procedure for the preparation of Ln1 complexes

The ligand was dissolved in methanol (5 mL) followed by an equimolar quantity of the appropriate lanthanide chloride in aqueous solution (3 mL) and the pH adjusted to pH 5.5 by addition of a solution of aqueous NaOH. The reaction was stirred at 50 °C for 48 hours after which the solvents were slowly evaporated slowly to dryness by heating at 80 °C. The solid residue was taken up into water (5mL) and was filtered through a 2 μm membrane filter. Lyophilization of the resulting solution afforded the Ln**1** complexes which were used without further purification.

Results and Discussion

All ligands were prepared according to the same general approach (Scheme 1). The appropriate butylamine was condensed with bromoacetyl bromide in dichloromethane at 0 °C, using potassium carbonate as a base. The resulting bromoacetamide was then used to alkylate cyclen in acetonitrile at 65 °C, again with potassium carbonate as a base. After recrystallization of the ligand from acetonitrile the lanthanide complexes were prepared by reacting equimolar amounts of ligand and the appropriate lanthanide chloride hexahydrate in water and adjusting the pH to 5.5 with NaOH solution.

Complexes of each ligand were prepared with all the paramagnetic Ln^{3+} ions, except Pm^{3+} and Gd^{3+}, and the SAP:TSAP ratio determined from the ^{1}H NMR spectra acquired in D_2O. In the complexes of the achiral ligands *tert*-**1**, *iso*-**1** and *n*-**1**, the two stereoisomers of each coordination geometry (Δ(λλλλ) and Λ(δδδδ) for SAP, and Δ(δδδδ) and Λ(λλλλ) for TSAP) are enantiomers. As a result two species, corresponding to the SAP and TSAP isomers, are observed in the ^{1}H NMR spectra of these complexes. Isomer interchange rates that were faster than the slow exchange limit were observed for the complexes Nd^{3+} and Sm^{3+} with all three ligands, and the Pr^{3+} complexes of iso-**1** and *tert*-**1**, leading to single broad lines for each resonance. Even upon cooling to 4 °C separate resonances for the two isomers could not be resolved, preventing determination of the isomeric ratios in these complexes. However, an approximate ratio can be estimated from the trend across the Ln^{3+} series. The mole fractions of the SAP and TSAP isomers of Ln*n*-**1** and Ln*iso*-**1** complexes across the Ln^{3+} series (Figure 1) show broadly similar trends. As with the Ln^{3+} complexes of DOTAM[32] the TSAP isomer is preferred exclusively for complexes of Ce^{3+} at the beginning of the Ln^{3+} series. The amount of SAP isomer observed in solution for all three butyl amide systems increases rapidly as the ionic radius of the Ln^{3+} ion gets smaller, although not as rapidly as for DOTAM complexes. However, it is with the later Ln^{3+} ions that the largest deviation from the behaviour of DOTAM complexes occurs. When the ionic radius reaches ~114.4 pm, at about Er^{3+}, DOTAM adopts the SAP isomer almost exclusively and remains in this geometry even as the ionic radius is

decreased further. Ln(*n*-**1**) and Ln(*iso*-**1**) complexes also reach a maximum population of SAP isomer in solution at about the same point, Er^{3+}, although the amount of SAP isomer varies depending upon the regiochemistry of the butyl group. However, in contrast to LnDOTAM complexes, after this point the amount of TSAP isomer present begins to increase again with decreasing Ln^{3+} ionic radius. The trend observed for Ln(*tert*-**1**) differs from those of its regioisomers; although it broadly follows the trend of the two other complexes for the early lanthanides it reaches a maximum SAP population at Dy^{3+} (ionic radius 116.7 pm) (Figure 1). Progressing through the later Ln^{3+} ions the TSAP becomes much more favored than in Ln (*n*-**1**) or Ln(*iso*-**1**) complexes, eventually becoming the predominant species of the Tm^{3+} and Yb^{3+} complexes. Notably the Ho^{3+} complex lies considerably outside this trend, adopting the TSAP isomer to a larger extent than predicted by the trend across the series. As yet this observation has not been rationalized.

The trend observed here in which the complexes of later Ln^{3+} ions increasingly favor the TSAP isomer with decreasing ionic radius is also observed for LnDOTA complexes[30] and has been ascribed to loss of the coordinating water molecule in the TSAP isomer.[28, 30] In principle the hydration state of an Yb^{3+} chelate can be determined by comparing the luminescent decay constant of Yb^{3+} in H_2O and D_2O.[37, 38] However, to date our attempts to determine the hydration state of Yb*tert*-**1** by luminescence were frustrated by high levels of scattering that made the measurement of emission from Yb^{3+} impossible. Nonetheless, it seems reasonable to assume that, even though this loss of water is not observed in the DOTAM complexes of the later Ln^{3+} ions, the TSAP isomers of achiral Ln**1** complexes with later Ln^{3+} ions are also without a coordinated water molecule. Clearly the nature of the amide substituent plays a role in determining this factor. It seems likely that two phenomena combine to drive this change in isomerization. Firstly, increased steric bulk in proximity to the coordinating amide function drives the complex into the more open TSAP geometry which better accommodates the bulky substituents. Secondly, increasing electron donating capacity of the butyl group, *tert*- > *iso*- > *n*-, results in increased provision of electron density to the Ln^{3+} by the amide ligands. It has previously been demonstrated that the electron density on the Ln^{3+} can be changed by the electronic properties of the amide substituent which in turn alters the demand for electron density from the coordinated water molecule.[39] Reducing this demand for electron density through electron donating amide substituents would allow the complex to adopt the TSAP geometry in which the water molecule is absent.

In contrast to the complexes of the achiral ligands, the ^1H NMR spectra of the complexes of *RRRR-sec*-**1** exhibit four species in solution. Each species is populated to a different extent and from the chemical shifts it appears that two of these species are SAP coordination geometries and the other two TSAP geometries. The observation of four stereoisomers in the ^1H NMR spectra of symmetrical DOTA-tetraamide complexes with chiral centres in the δ-position is unusual. In DOTA-tetraamide complexes derived from alanine and its esters,[40, 41] and from α-methylbenzyl amine,[42] only one species is observed in solution. In each case the coordination geometry of the solitary species has been identified as the SAP isomer. From crystallographic data it is apparent that the configuration of the chiral centre in the δ-position controls the orientation of the pendant arms in much the same way that α-substitution controls the orientation of the pendant arms in tetraacetate complexes.[23–25, 43, 44] α-Substitution is a particularly effective way of determining the orientation of pendant arms since the steric and torsional strain of placing the substituent in a *gauche* position, relative to the metal ion, is highly disfavored (Figure 2 top). This leads to an *R*- configuration conferring a Λ orientation and *S*- a Δ orientation on the pendant arms.[23, 43] In the crystal structures of DOTA-tetraamide complexes with bulky substituents such as benzyl or a carboxylate ester, at δ-chiral centers the bulky group is invariably in a pseudo-equatorial position (Figure 2 bottom).[40–42, 45] Arm rotation would place the bulky group in a pseudo-axial position which is presumably of higher energy and therefore disfavored. Thus, bulky δ-substitutents appear to effectively freeze-out

arm rotation with the same relationship between configuration at carbon and pendant arm orientation observed for the α-substituent systems. Because the orientation of the pendant arms is fixed only two of the four stereoisomeric coordination isomers are accessible, one SAP and one TSAP. Of these only the SAP isomer is actually observed presumably as a result of the unexplained preference for this isomer in complexes with large amide substituents that was discussed earlier.

It is worthy of note that in DO3A-triamide complexes with chiral centres in the δ-position the bulky group of the chiral centre can be induced to adopt a pseudo-axial position. When a ternary complex is formed between the complex and a second chiral ligand, if the chirality of the second ligand is such that it forces the pendant arms into the conformation normally opposed by the δ- chiral center then the bulky group is forced into the pseudo-axial position.[46, 47] This seems to indicate that although the pseudo-axial position is higher in energy than the pseudo-equatorial position it is nonetheless accessible. This is apparent in the NMR spectrum of Yb*RRRR-sec*-**1** (Figure 3) in which all four possible coordination stereoisomers are observed. The ethyl group, the largest of the chiral substituents in this complex, is clearly not sufficiently bulky to demand the pseudo-equatorial position exclusively. As a result arm rotation can still occur freely as demonstrated by the EXSY spectrum of the complex.

EXSY is a well established method of examining the intramolecular motions in these types of complex. By following the possible exchange pathways of the protons of the coordination cage - the macrocyclic and acetamide protons - it is possible to establish which processes are taking place within a complex. The EXSY spectrum of Yb*RRRR-sec*-**1** is shown in Figure 4. Each resonance corresponding to a proton of the coordination cage correlates to three cross-peaks. These cross-peaks correlate in turn with a resonance from each of the other three isomers. By comparing the shift data with that of related Yb^{3+} complexes and from the COSY data (supplementary information S1) it is possible to assign the protons of the coordination cage in each of the four isomers. Examination of the cross-peaks related to the macrocyclic protons in the EXSY spectrum identifies three intramolecular motions:

Arm rotation	SAP↔TSAP	$ax^S \leftrightarrow eq^C$, $ax^C \leftrightarrow eq^S$
Ring flip	SAP↔TSAP	$ax^S \leftrightarrow ax^S$, $ax^C \leftrightarrow ax^C$, $eq^S \leftrightarrow eq^S$, $eq^C \leftrightarrow eq^C$
Sequential ring flip and arm rotation	SAP↔SAP TSAP↔TSAP	$ax^S \leftrightarrow eq^C$, $ax^C \leftrightarrow eq^S$

We can safely assume that the most favorable isomer will remain the one in which the orientation of the pendant arms places the ethyl substituent in the pseudo-equatorial position of a SAP isomer. In other words, for the *RRRR*- isomer of *sec*-**1** the major species would be expected to be the Λ(δδδδ) isomer (Figure 5). The major species in solution is indeed a SAP isomer and on the basis of this assignment we can conclude that the other SAP isomer Δ (λλλλ), which is obtained by arm rotation, has the ethyl groups in a pseudo-axial position. Notably this is the next most populated species in solution suggesting that the driving force for adopting a SAP isomer is more powerful than that which places bulky substituents into pseudo-equatorial positions. Ring flip of the Λ(δδδδ) major isomer, which affords the TSAP Λ(λλλλ) structure, would allow the ethyl groups to remain in a pseudo-equatorial position because the orientation of the pendant arms is not changed by this motion. Surprisingly this is not the major TSAP species in solution. Rather the Δ(δδδδ) isomer is found to be the favored TSAP isomer but this structure would seem to place the ethyl substituents in a pseudo axial position since it is obtained by sequential ring flip and arm rotation of the major Λ(δδδδ) species. This phenomenon is particular to the very heaviest Ln^{3+} ions. An EXSY spectrum of Eu*sec*-**1** (data not shown) reveals that the major SAP isomer Λ(δδδδ) undergoes a ring flip

conversion with the major TSAP isomer, not the minor TSAP isomer as observed with Yb^{3+}. That means unlike the Yb^{3+} complex the major TSAP isomer of Eu*sec*-**1** is the Λ(λλλλ) isomer.

Figure 6 shows the ^{1}H NMR spectrum, focussed on the most shifted axial proton ax^{S}, of each Ln(*sec*-**1**) complex in which the resonances of each isomer can be clearly seen. The total SAP/total TSAP ratio broadly follows the trend observed for the other regioisomeric Ln**1** complexes; the TSAP isomer is observed exclusively for the earliest lanthanides, $Ce^{3+} \rightarrow Nd^{3+}$, thereafter the SAP isomer becomes increasingly favored until it reaches a maximum at Tm^{3+}. Then on passing to Yb^{3+}, the total population of TSAP isomer increases again at the expense of the SAP isomers. Underlying this broader trend is the intriguing relationship between the two diastereoisomers of each coordination geometry. The relationship of the two SAP isomers remains fairly constant across the series. The major SAP isomer is always the less shifted isomer and as discussed previously this represents the Λ(δδδδ) isomer in which the bulky group is in a pseudo-equatorial position. The ratio of the Λ(δδδδ) (major) and Δ(λλλλ) (minor) isomers remains broadly similar across the series, although this ratio does tighten slightly around Dy^{3+}. The relationship between the two TSAP isomers is, by comparison, more complicated. From the EXSY data acquired on Eu(*sec*-**1**) and Yb(*sec*-**1**) the less shifted isomer is readily assigned to the Λ(λλλλ) isomer. The relative population of this isomer changes from the major TSAP isomer across the first half of the Ln^{3+} series, to the minor isomer for Tm^{3+} and Yb^{3+}. From the trends across the series it is apparent that the Λ(λλλλ) isomer becomes the minor isomer between Er^{3+} and Tm^{3+}. Notably for these two Ln^{3+} ions only one TSAP isomer is observed; for Er^{3+} this is the Λ(λλλλ) isomer the relative population of which is decreasing at this point in the series minimizing at Tm^{3+}. The Δ(δδδδ) minimizes at Er^{3+} and is the single TSAP isomer observed for Tm^{3+} and the major TSAP isomer thereafter. This switch in the relative populations of the two TSAP isomers, which coincides with the beginning of increased favorability of TSAP isomers generally, indicates that the position of the bulky substituent and accommodating an inner-sphere water molecule are interrelated. It appears departure of the inner-sphere water molecule favours rotating the arms to place the bulky substituent into the normally less stable pseudo-axial position. Exactly why this should be remains unclear and, in the absence of more crystallographic data, is likely to remain so.

Conclusions

The four regioisomeric complexes of DOTA-tetrabutylamides **1** provide a fascinating insight into the factors that govern the coordination geometry and conformation in this class of Ln^{3+} complex. Although TSAP isomers are preferred for the earliest and largest Ln^{3+} ions, the isomeric ratios observed for later Ln^{3+} ions do not parallel those observed for LnDOTAM complexes.[32] The SAP isomers do become progressively more favorable as the lanthanide ionic radius decreases but for each regioisomer a point is reached at which this trend reverses and the TSAP isomers become increasingly populated. That point is dependent upon the regiochemistry of the butyl amide substituent and is presumably related to the changing steric and electronic properties of regioisomeric butyl groups. The rise in the TSAP isomer populations at the end of the Ln^{3+} series appears to arise from the loss, or partial loss,[38] of the coordinated water molecule in a manner similar to that observed for LnDOTA complexes.[28, 30]

By far the most interesting regioisomer studied herein are the Ln(*sec*-**1**) complexes. The introduction of a chiral center in the amide substituent renders all four possible coordination modes diastereoisomeric. Unusually, all four of these coordination isomers can be observed in solution. Contrary to the conclusion that might reasonably be reached from studying systems with large substituents and δ-chiral centers,[40–42, 45] this complex shows that chiral centers in the δ-position are not a guaranteed method of controlling the helicity of pendant arms in DOTA-tetraamide complexes. Curiously, it is observed that for the smallest lanthanide ions, Tm^{3+} and

Yb^{3+}, the arrangement of the substituents in the major TSAP isomer is contrary to that expected for the lowest energy. We hypothesize that the larger substituent is placed in the pseudo-axial position to better accommodate the substituent when the complex loses its inner sphere water molecule.

Supplementary Material

Refer to Web version on PubMed Central for supplementary material.

Acknowledgments

The authors thank the National Institutes of Health (RR-02584, CA-126608 and CA-115531), the Robert A Welch Foundation (AT-584) and the University of Texas at Dallas for financial assistance.

Notes and References

1. Caravan P, Ellison JJ, McMurry TJ, Lauffer RB. Chem. Rev 1999;99(9):2293–2352. [PubMed: 11749483]
2. Toth, E.; Merbach, AE. Chemistry of Contrast Agents in Medical Magnetic Resonance Imaging. New York: Wiley; 2001.
3. Aime S, Barge A, Botta M, De Sousa AS, Parker D. Angew. Chem. Int. Ed 1998;37(19):2673–2675.
4. Aime S, Barge A, Botta M, Parker D, De Sousa AS. J. Am. Chem. Soc 1997;119(20):4767–4768.
5. Aime S, Barge A, Bruce JI, Botta M, Howard JAK, Moloney JM, Parker D, de Sousa AS, Woods M. J. Am. Chem. Soc 1999;121(24):5762–5771.
6. Woods M, Woessner Donald E, Sherry AD. Chem Soc Rev 2006;35(6):500–511. [PubMed: 16729144]
7. Zhang S, Winter P, Wu K, Sherry AD. J. Am. Chem. Soc 2001;123(7):1517–1518. [PubMed: 11456734]
8. Zhang S, Michaudet L, Burgess S, Sherry AD. Angew. Chem. Int. Ed 2002;41(11):1919–1921.
9. Aime S, Barge A, Castelli DD, Fedeli F, Mortillaro A, Nielsen FU, Terreno E. Magn. Reson. Med 2002;47(4):639–648. [PubMed: 11948724]
10. Aime S, Castelli DD, Terreno E. Angew. Chem., Int'l. Ed 2002;41(22):4334–4336.
11. Zhang S, Merritt M, Woessner DE, Lenkinski RE, Sherry AD. Acc. Chem. Res 2003;36(10):783–790. [PubMed: 14567712]
12. Zhang S, Trokowski R, Sherry AD. J. Am. Chem. Soc 2003;125(50):15288–15289. [PubMed: 14664562]
13. Terreno E, Castelli Daniela D, Cravotto G, Milone L, Aime S. Invest. Radiol 2004;39(4):235–243. [PubMed: 15021328]
14. Trokowski R, Zhang S, Sherry AD. Bioconjug. Chem 2004;15(6):1431–1440. [PubMed: 15546212]
15. Aime S, Carrera C, Delli Castelli D, Geninatti Crich S, Terreno E. Angew. Chem., Int'l. Ed 2005;44(12):1813–1815.
16. Trokowski R, Ren JM, Kalman FK, Sherry AD. Angew. Chem. Int'l. Ed 2005;44(42):6920–6923.
17. Zhang S, Malloy CR, Sherry AD. J. Am. Chem. Soc 2005;127(50):17572–17573. [PubMed: 16351064]
18. Suchy M, Li AX, Bartha R, Hudson RHE. Bioorg. Med. Chem 2008;16(11):6156–6166. [PubMed: 18457955]
19. Li AX, Wojciechowski F, Suchy M, Jones CK, Hudson RHE, Menon RS, Bartha R. Magn. Reson. Med 2008;59(2):374–381. [PubMed: 18228602]
20. Wojciechowski F, Suchy M, Li AX, Azab HA, Bartha R, Hudson RHE. Bioconjug. Chem 2007;18(5):1625–1636. [PubMed: 17711349]
21. Woessner DE, Zhang S, Merritt ME, Sherry AD. Magn. Reson. Med 2005;53(4):790–799. [PubMed: 15799055]
22. Dunand FA, Aime S, Merbach AE. J. Am. Chem. Soc 2000;122(7):1506–1512.

23. Woods M, Aime S, Botta M, Howard JAK, Moloney JM, Navet M, Parker D, Port M, Rousseaux O. J. Am. Chem. Soc 2000;122(40):9781–9792.
24. Woods M, Kovacs Z, Zhang S, Sherry AD. Angew. Chem. Int'l. Ed 2003;42(47):5889–5892.
25. Woods M, Botta M, Avedano S, Wang J, Sherry AD. Dalton Trans 2005;(24):3829–3837. [PubMed: 16311635]
26. Marques MPM, Geraldes CFGC, Sherry AD, Merbach AE, Powell H, Pubanz D, Aime S, Botta M. J. Alloys Compounds 1995;225(1–2):303–307.
27. Aime S, Botta M, Ermondi G. Inorg. Chem 1992;31(21):4291–4299.
28. Benetollo F, Bombieri G, Calabi L, Aime S, Botta M. Inorg. Chem 2003;42:148–157. [PubMed: 12513089]
29. Hoeft S, Roth K. Chem. Ber 1993;126(4):869–873.
30. Aime S, Botta M, Fasano M, Marques MPM, Geraldes CFGC, Pubanz D, Merbach AE. Inorg. Chem 1997;36(10):2059–2068. [PubMed: 11669824]
31. Jacques V, Desreux JF. Inorg. Chem 1994;33(18):4048–4053.
32. Vipond J, Woods M, Zhao P, Tircso G, Ren JM, Bott SG, Ogrin D, Kiefer GE, Kovacs Z, Sherry AD. Inorg. Chem 2007;46(7):2584–2595. [PubMed: 17295475]
33. Woods M, Kovacs Z, Kiraly R, Bruecher E, Zhang S, Sherry AD. Inorg. Chem 2004;43(9):2845–2851. [PubMed: 15106971]
34. Woods M, Zhang S, Von Howard E, Sherry AD. Chem. Eur. J 2003;9(19):4634–4640.
35. Zhang S, Wu K, Biewer MC, Sherry AD. Inorg. Chem 2001;40(17):4284–4290. [PubMed: 11487334]
36. Zhang S, Jiang X, Sherry AD. Helv. Chim. Acta 2005;88(5):923–935.
37. Faulkner S, Beeby A, Dickins RS, Parker D, Williams JAG. J. Fluoresc 1999;9(1):45–49.
38. Beeby A, Clarkson IM, Dickins RS, Faulkner S, Parker D, Royle L, de Sousa AS, Williams JAG, Woods M. J. Chem. Soc., Perkin Trans. 2 1999;(3):493–504.
39. Ratnakar SJ, Woods M, Lubag AJM, Kovacs Z, Sherry AD. J. Am. Chem. Soc 2008;130(1):6–7. [PubMed: 18067296]
40. Aime S, Barge A, Botta M, Howard JAK, Kataky R, Lowe MP, Moloney JM, Parker D, de Sousa AS. Chem. Commun 1999;(11):1047–1048.
41. Gunnlaugsson T, Davies RJH, Nieuwenhuyzen M, O'Brien JE, Stevenson CS, Mulready S. Polyhedron 2003;22(5):711–724.
42. Dickins RS, Howard JAK, Lehmann CW, Moloney J, Parker D, Peacock RD. Angew. Chem. Int. Ed 1997;36(5):521–523.
43. Howard JAK, Kenwright AM, Moloney JM, Parker D, Woods M, Port M, Navet M, Rousseau O. Chem. Commun 1998;(13):1381–1382.
44. Di Bari L, Pintacuda G, Salvadori P. Eur. J. Inorg. Chem 2000;(1):75–82.
45. Dickins RS, Howard JAK, Maupin CL, Moloney JM, Parker D, Riehl JP, Siligardi G, Williams JAG. Chem. Eur. J 1999;5(3):1095–1105.
46. Dickins RS, Aime S, Batsanov AS, Beeby A, Botta M, Bruce JI, Howard JAK, Love CS, Parker D, Peacock RD, Puschmann H. J. Am. Chem. Soc 2002;124(43):12697–12705. [PubMed: 12392417]
47. Dickins RS, Batsanov AS, Howard JAK, Parker D, Puschmann H, Salamano S. Dalton Trans 2004;(1):70–80. [PubMed: 15356744]

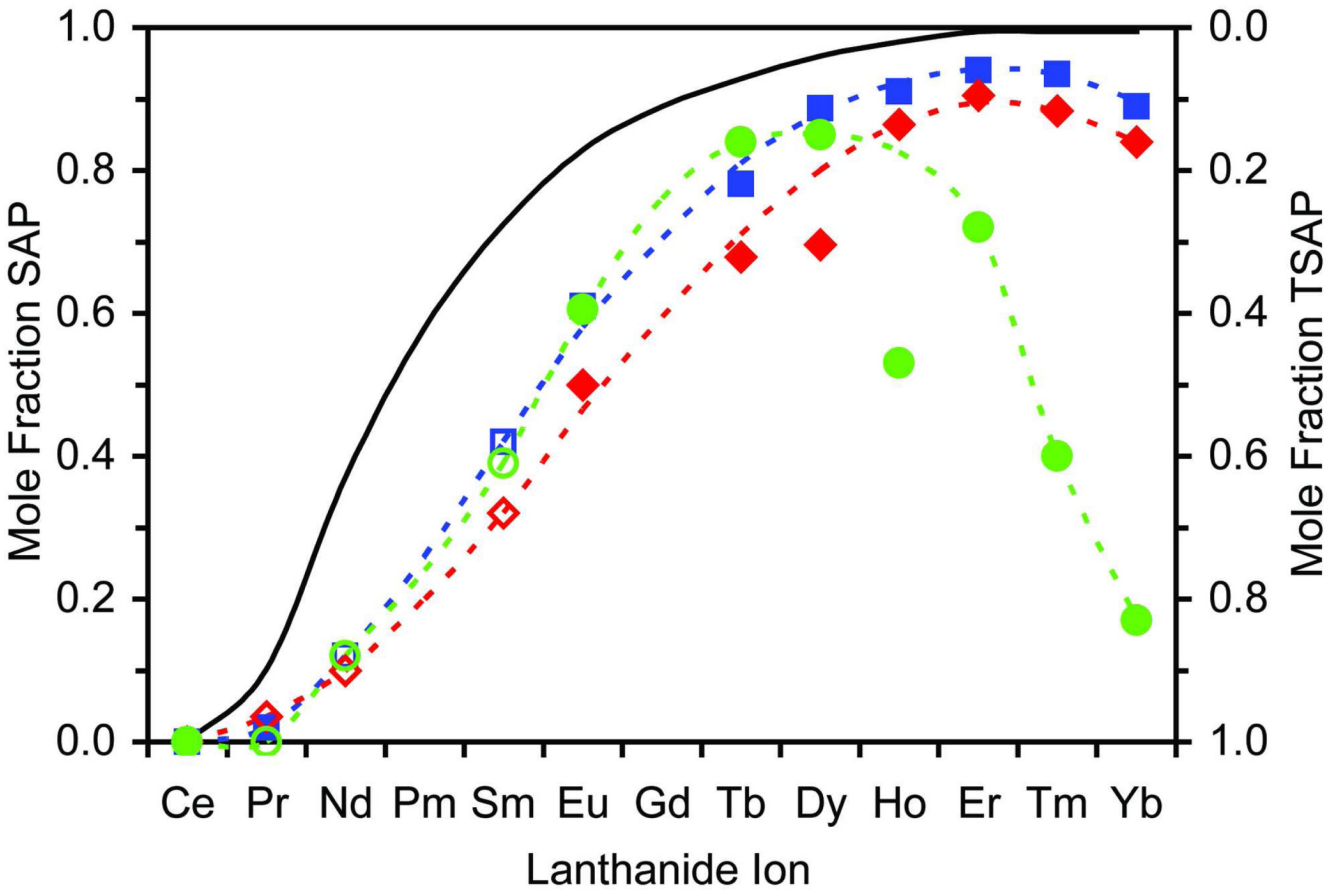

Figure 1.

The mole fractions of the SAP (left axis) and TSAP (right axis) isomers of *tert*-**1** (green circles), *iso*-**1** (red diamonds) and *n*-**1** (blue squares) across the lanthanide series. Filled symbols are experimentally determined values whereas open symbols indicate that the mole fractions are an estimate based upon the trend across the series. The dashed trend lines are solely for the purposes of guiding the eye. The solid black line shows the trend observed for DOTAM complexes.[32]

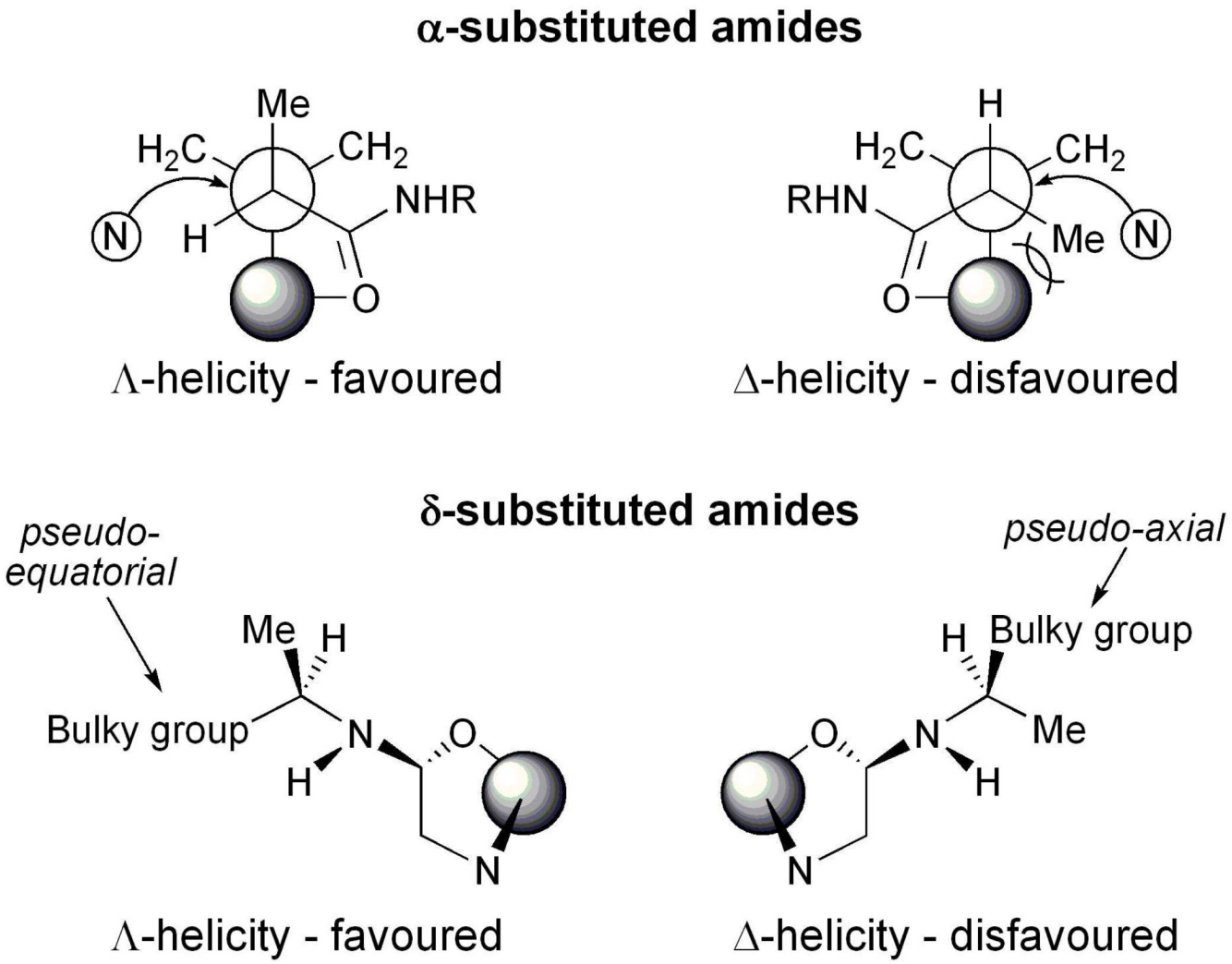

Figure 2.

In α-substituted pendant arms the substituent is preferentially orientated *anti*- to the metal ion, looking down the N-C_α bond (top). In δ-substituted arms with bulky groups, such as benzyl, carboxylates or carboxylate esters, the bulky group preferentially adopts a pseudo-equatorial position (bottom left). Arm rotation would force the bulky group into a pseudo-axial position which, from NMR data, appears to be unfavourable for large groups (bottom right). In all cases an *R*- configuration of the chiral center is shown.

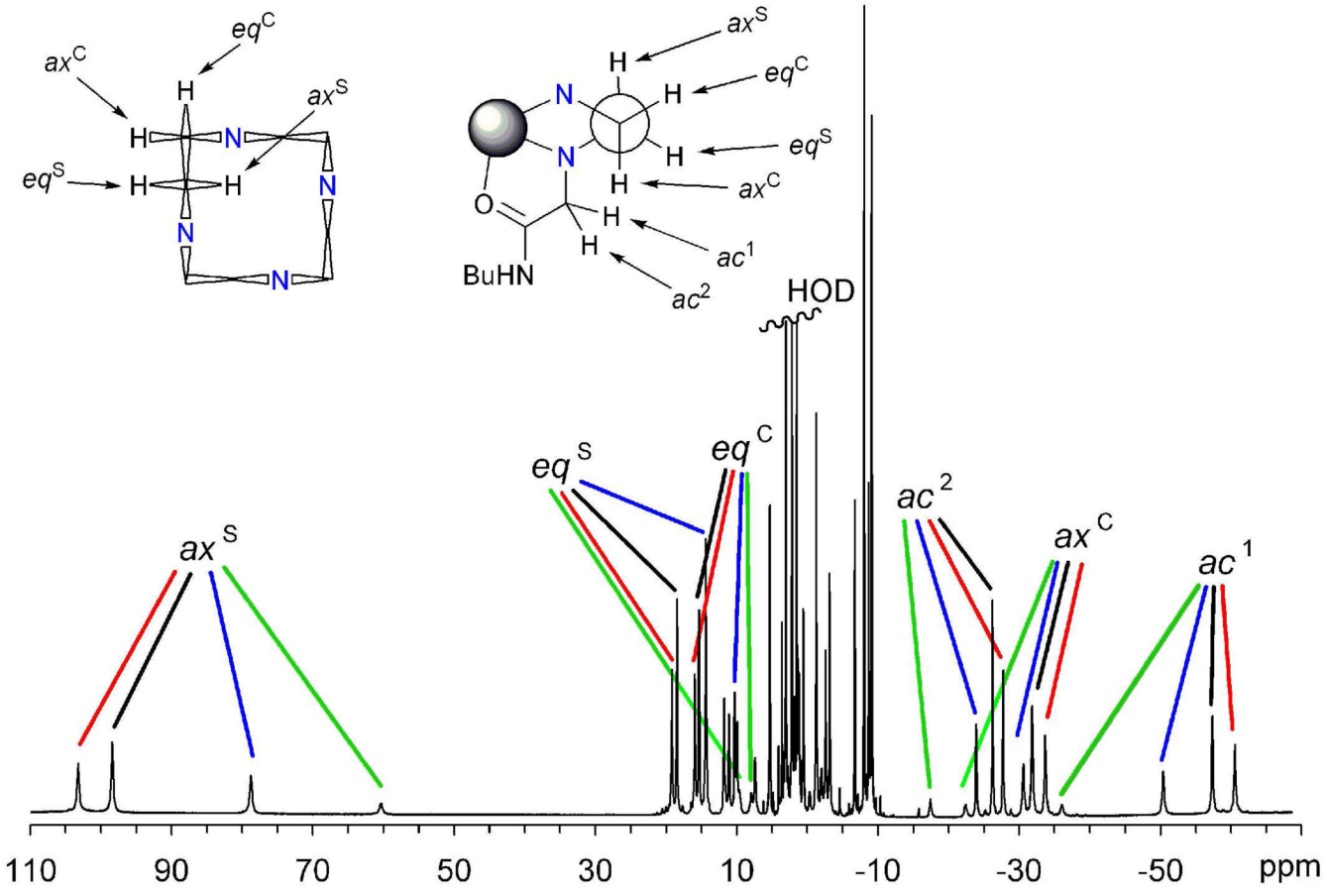

Figure 3.

^{1}H NMR spectrum of Yb*RRRR-sec*-**1** recorded at 500 MHz and 298K in D_2O (pD 7.41). The peaks corresponding to the coordination cage (the macrocyclic ring and acetamide protons) in the spectrum of each coordination isomer have been assigned according to the following scheme: Δ(λλλλ) (SAP), red; Λ(δδδδ) (SAP), black; Δ(δδδδ) (TSAP), blue; and Λ(λλλλ) (TSAP), green. The notation scheme *ax* for an axial proton, *eq* for an equatorial proton and *ac* for acetamide proton has been used. The superscript S and C denote the position of the proton on the macrocycle, on the side or on the corner, respectively. Protons from the butyl groups have not been assigned.

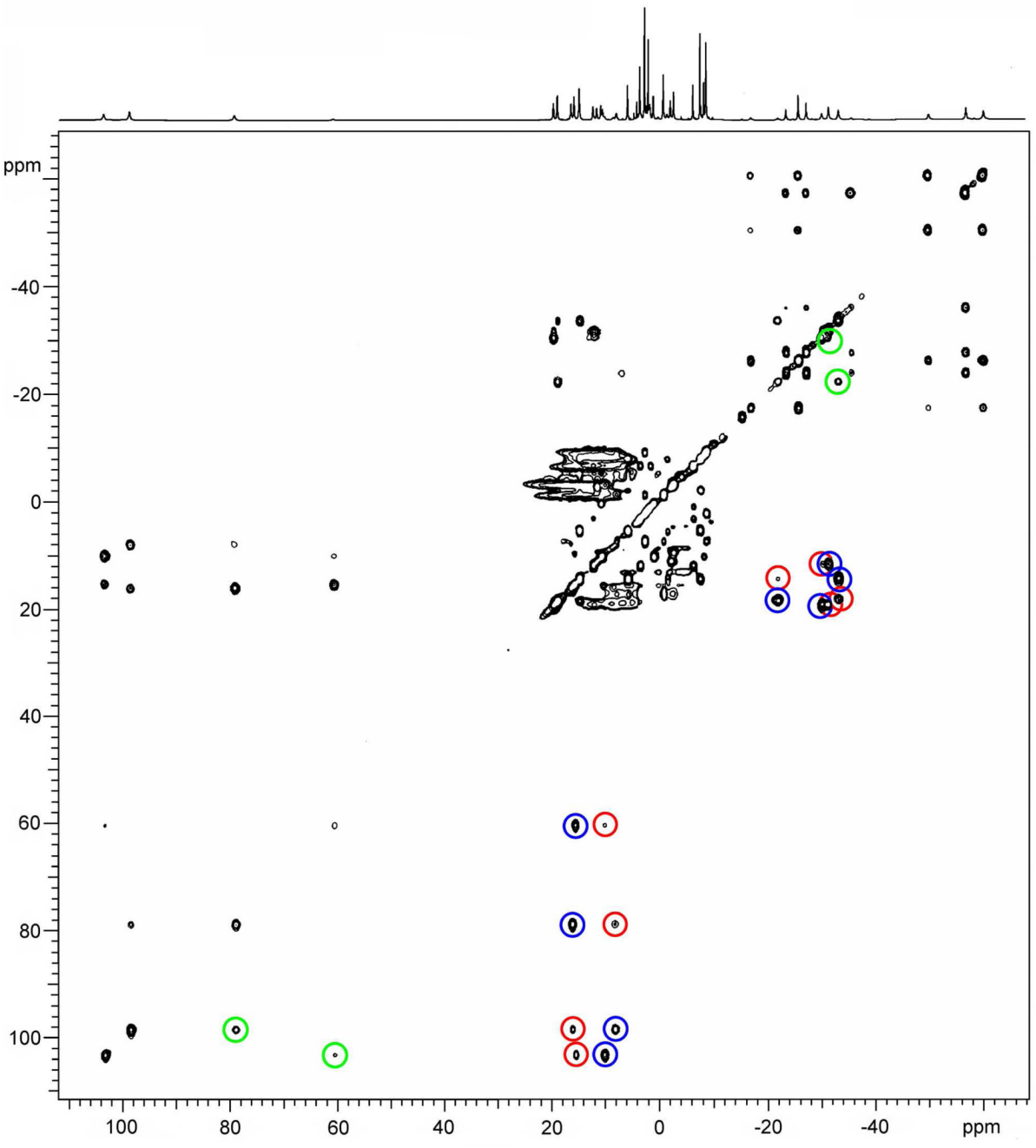

Figure 4.

The ^{1}H EXSY spectrum of Yb*RRRR-sec*-**1** recorded at 500 MHz and 298 K in D_2O (pD 7.41). Cross-peaks that correspond to ring flip are labelled in blue, those that correspond to arm rotation in green and those that correspond to sequential ring flip and arm rotation in red. The cross-peaks that correspond to the trans position of equatorial protons by arm rotation have not been labelled as they lie in the cluttered region in the center of the spectrum that is also subject to significant T_1 noise.

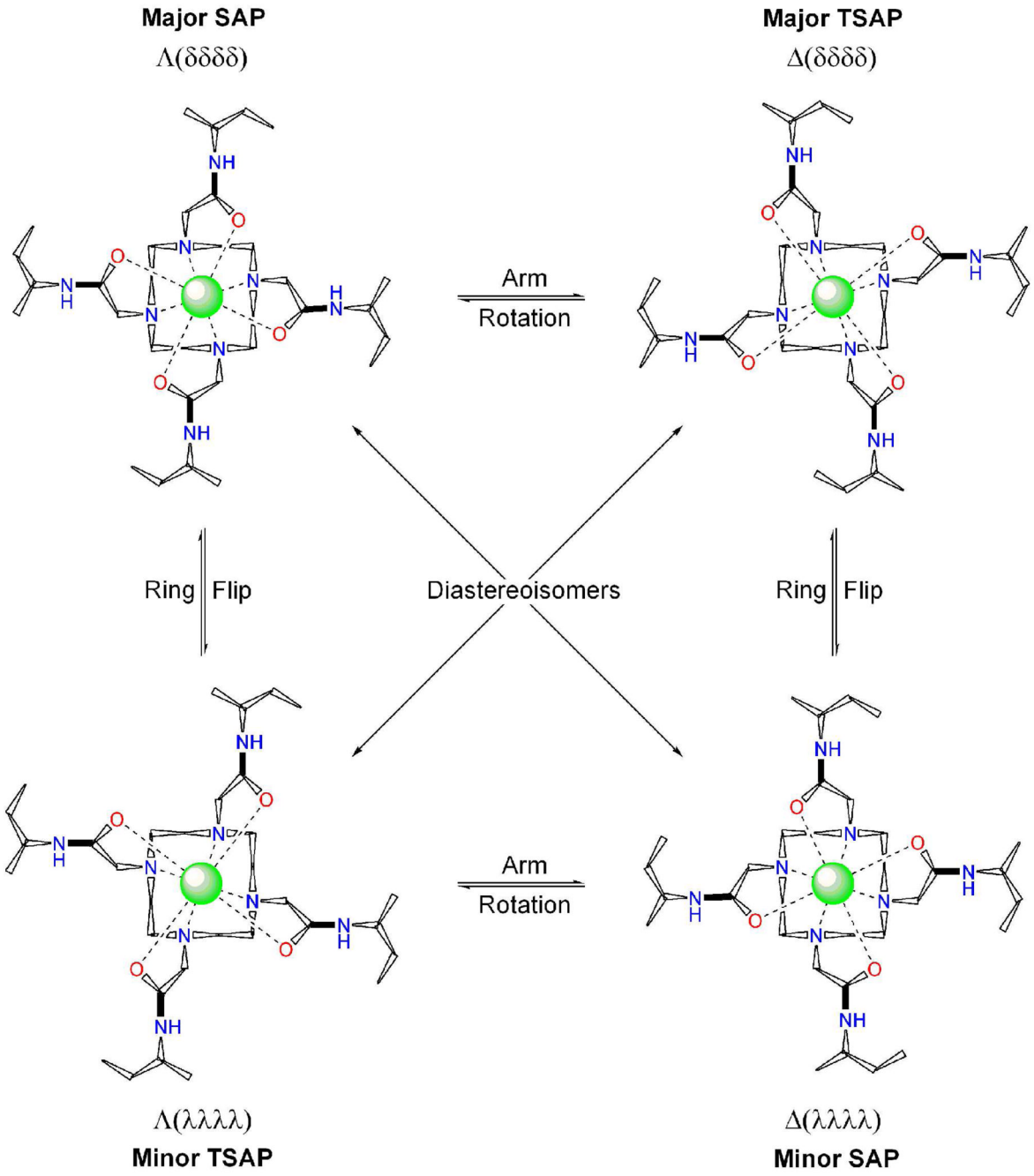

Figure 5.

A schematic representation of the four stereoisomers of Ln*RRRR-sec*-**1**. The complexes are shown looking down the H_2O-Ln bond, macrocycle to the back. The coordinated water molecule has been omitted for clarity.

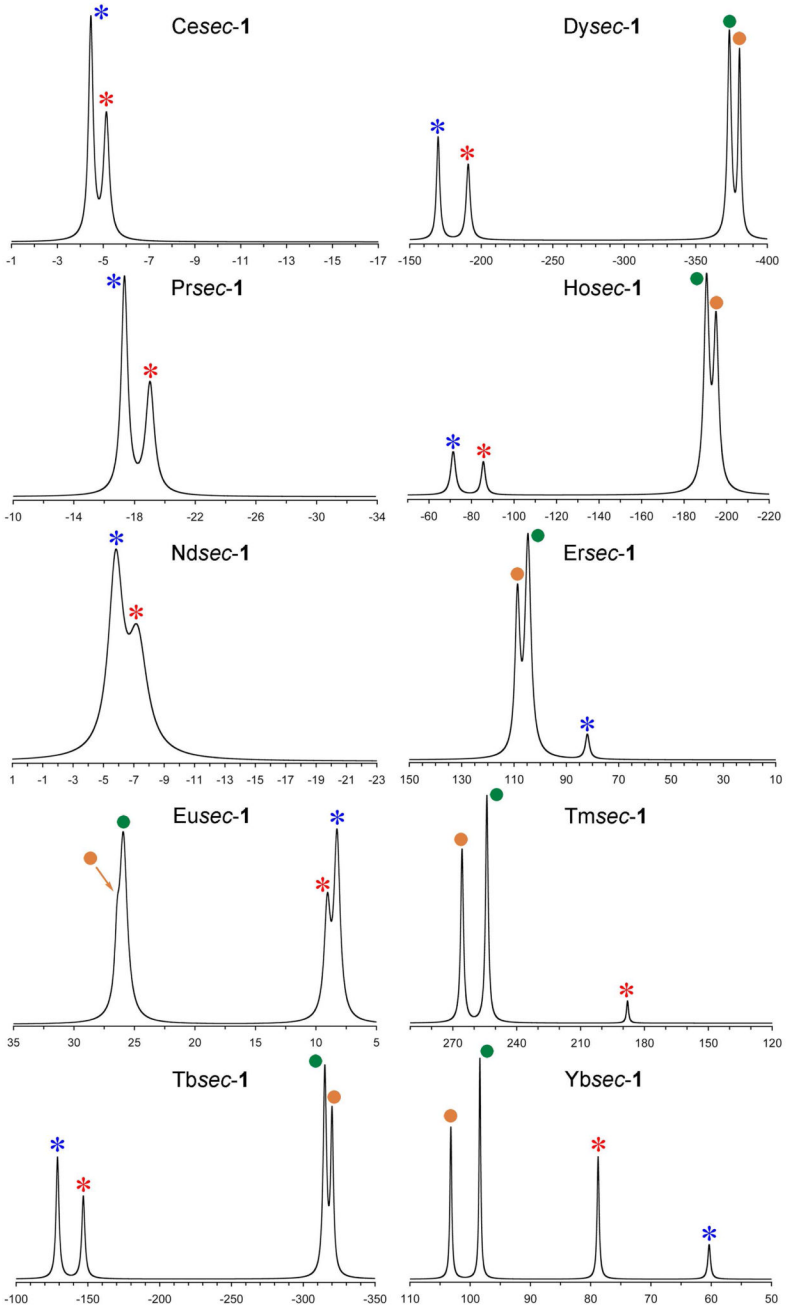

Figure 6.

^{1}H NMR spectra, focussing on the *ax*^{S} proton (Figure 3), of Ln*RRRR-sec*-**1** complexes recorded in D_2O, pD 7.4 across the rare earth series. Peaks corresponding to the SAP isomer are labelled with circles - Δ(λλλλ) (orange) and Λ(δδδδ) (green) – and the TSAP isomers are labelled with asterisks - Δ(δδδδ) (red) and Λ(λλλλ) (blue). The assignment of the TSAP isomers of the TSAP isomers of Er *RRRR-sec*-**1** and Tm *RRRR-sec*-**1** are based upon the observed trend across the later Ln series in which the mole fraction of the Δ(δδδδ) isomer decreases more quickly than that of the Λ(λλλλ). Clealry then, the proportion of the Δ(δδδδ) isomer present will increase more quickly as the ionic radius is further decreased as evidenced by the isomeric assignment for Yb*RRRR-sec*-**1**.

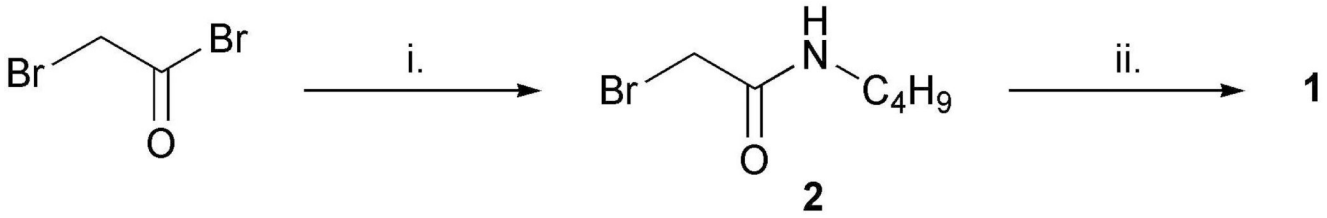

Scheme 1.

The synthesis of the DOTA-tetraamides **1**. Reagents and conditions: i. $H_2NC_4H_9$ / K_2CO_3 / CH_2Cl_2 / 0 °C; ii. Cyclen / K_2CO_3 / MeCN/ 65 °C.

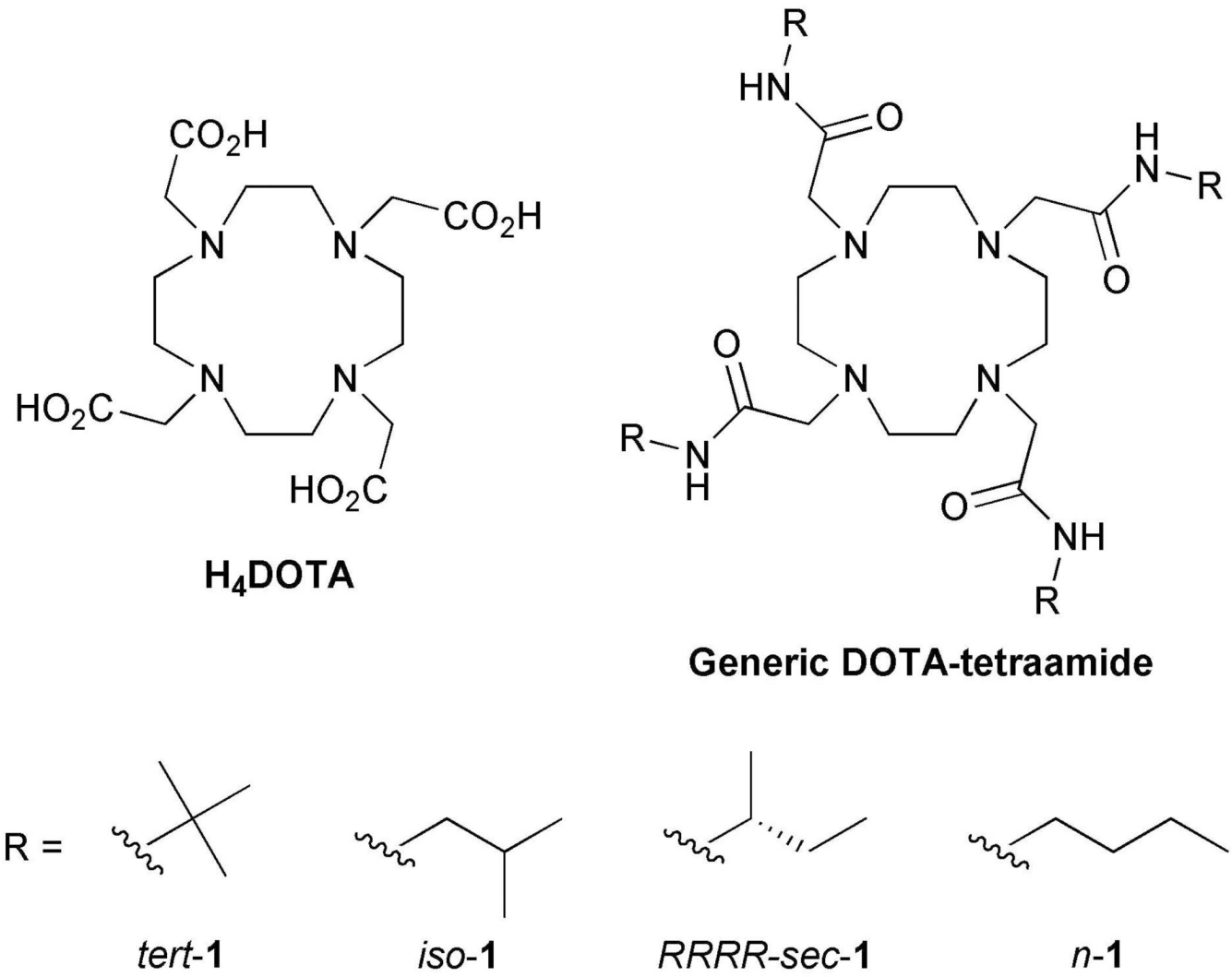

Chart 1.
The structures of DOTA and the four DOTA-tetraamide ligands derived from the four regioisomers of aminobutane.